Beta Phase Crystallization and Ferro/Piezoelectric Performances of Melt-Processed PVDF Blends with PMMA Copolymers Containing Ionizable Moieties

Alexandre De Neef[1,2], Cédric Samuel[2], Harvey Amorín[3], Gregory Stoclet[4], Ricardo Jiménez Rioboo[3], Philippe Dubois[1], Jérémie Soulestin[2], Jean-Marie Raquez[1]*

[1] University of Mons (UMons), Laboratory of Polymeric and Composite Materials (LPCM), Center of innovation and research in Materials and Polymers (CIRMAP), Place du Parc 23, B-7000 Mons, Belgium.

[2] Ecole Nationale Supérieure Mines Telecom Lille Douai, Institut Mines Telecom Lille Douai (IMT Lille Douai), Département Technologie des Polymères et Composites & Ingénierie Mécanique (TPCIM), Cité Scientifique, Rue Guglielmo Marconi, F-59650 Villeneuve-d'Ascq, France.

[3] Instituto de Ciencia de Materiales de Madrid (ICMM), Consejo Superior de Investigaciones Científicas (CSIC), Cantoblanco, 28049 Madrid, Spain

[4] Université de Lille, CNRS, INRAE, Centrale Lille, UMR 8207 – UMET – Unité Matériaux et Transformations (UMET), F-59000 Lille, France

Keywords. Poly(vinylidene difluoride), Poly(methyl methacrylate), Polymer Blends, Extrusion, Piezoelectrics, Ferroelectrics.

Abstract. Poly(methyl methacrylate-*co*-methacrylic acid) (PMMA-*co*-MAA) copolymer containing ionizable moieties is here investigated as a melt processing additive for PVDF to develop high-quality ferro/piezoelectric polymer films by extrusion-calendering. The PVDF/PMMA-*co*-MAA miscibility and the β-phase crystallization from the melt state at high cooling rates were first explored by Flash DSC. Transposition to the melt-processing of thin films by extrusion-calendering is attempted and a direct production of β-crystals in high amounts is attested at a specific content of 5 wt-% PMMA-*co*-MAA. Ferro/piezoelectric properties were subsequently investigated and classical ferroelectric-type hysteresis loops clearly appear at room temperature for AC electric fields higher than 900 – 1200 kV/cm. Enhanced remanent polarizations (P_r) are observed with only 5 wt-% PMMA-based additives and the best ferroelectric performances are identified for PVDF/PMMA-*co*-MAA blends, in agreement with a higher β-phase content. Stable piezoelectric properties are also highlighted with maximal piezoelectric coefficient (d_{33}) of 11 pC/N for these formulations. A linear relationship is found between d_{33} and P_r in accordance with several models and, in this respect, the origin/optimization of the remanent polarization was investigated. Crystal transformations are revealed during high-voltage AC poling and high-quality ferroelectric behaviors with high P_r values up to 7 μC/cm² are obtained at elevated poling temperatures for PVDF/PMMA-*co*-MAA blends (theoretical d_{33} up to 16 pC/N) approaching the theoretical limit value for perfectly-poled β-crystals. This study clearly opens up interesting perspectives in the development of cost-effective electroactive polymer films using industrially-relevant processes and demonstrates that PVDF-based blends with miscible functional PMMA copolymers represent an interesting approach for this purpose.

1. Introduction

For decades, high interests have been observed for the implementation of poly(vinylidene fluoride) (PVDF) and its copolymers in the domain of ferro/piezoelectric materials[1–4]. Currently, ferroelectric and piezoelectric properties of PVDF-based materials are of great interest for flexible sensors, transducers and actuators[2–5] as well as for future prospects in many advanced applications such as energy harvesters/μ-generators[6,7], energy storage[8,9], random-access memories (FeRAMs)[10–12], artificial muscles for robotics and (bio)microelectronic devices[13].

The piezoelectric and ferroelectric properties of semi-crystalline PVDF arise from specific crystalline phases depending on the conformation of the CH_2-CF_2 linkages[1–4]. Among the 3 main crystalline phases of PVDF, the most thermodynamically stable is the so-called α-phase (form II, conformation TGTG')[1–4] that remains non-polar with a paraelectric dielectric behavior. Unfortunately, this non-polar phase is the most commonly produced during melt-state processing of PVDF. The other two phases are polar and of high interest for piezoelectric/ferroelectric properties, γ-phase (form III, conformation TTTGTTTG') and β-phase (form I, conformation 100% trans). This last conformation presents the highest dipolar moments, due to a regular arrangement of hydrogen and fluorine atoms in the opposite directions resulting in a large molecular dipolar moment oriented perpendicularly to the chain axis. The parallel orientation of all the monomers in the β-phase allows to reach large spontaneous/remanent polarizations of 6.5 – 9 μC/cm^2, giving a maximum piezoelectric coefficient d_{33} of approx. 35 pC/N[2–4,14–18]. The amorphous phase and crystal-amorphous interphase from PVDF could play an important role in its electroactive properties in particular in charge transfer/coupling between crystalline lamellae[19–21].

Unfortunately, the PVDF β-phase is difficult to obtain using a conventional melt-extrusion processing method and various approaches were developed. The most common route employed to get the PVDF β-phase is the uniaxial/biaxial stretching of PVDF films with a partial conversion of PVDF α-phase into the β-phase (efficiency close to 75 – 80%)[2,14,17]. The PVDF β-phase could also directly appear from the melt state using specific (nano)fillers[22–24] but conductive and non-polarizable PVDF materials are generally obtained that highly restrict their subsequent poling under very high voltage (> 500 kV/cm)[3,16,18,25]. Another alternative lies on the use of the poly(vinylidene fluoride-*co*-trifluoroethylene) copolymers, *i.e.* P(VDF-*co*-TrFE), that could directly develop the ferroelectric/piezoelectric crystal phase either from the melt state or from solvent casting[2]. Despite interesting ferroelectric performances with remanent polarizations up to 11 μC/cm², the use of P(VDF-*co*-TrFE) copolymers still faces several limitations. These copolymers display a ferroelectric - paraelectric crystal transitions at temperature down to 50 – 70°C (depending on the TrFE content) that could restrict high-temperature applications. The cost of such copolymer is also very restrictive for their large-scale applications using melt-state processes of the plastic industry and solvent-based processing methods such as spin coating are preferred. In this context, new approaches are required to reach high β-phase content using neat PVDF by environmental-friendly and cost-effective processes, in particular thin films extrusion processing.

Melt-blending PVDF with a miscible polymer was also found to promote PVDF crystallization into the β-phase from the melt-state due to specific interactions between PVDF and a (partially) miscible polymer. This is the case of poly(methyl methacrylate) (PMMA) with the occurrence of (i) dipole-dipole interactions between electrical moments of the carbonyl groups of PMMA and of the CF_2 groups of PVDF and (ii) specific H-bonding interactions between the carbonyl oxygens of

PMMA and CH_2 groups of PVDF[26]. An abundant literature regarding PVDF/PMMA miscibility, β-phase crystallization induced by PMMA and ferroelectric behavior for PVDF/PMMA blends[12,27–35] has already been reported. Briefly, using a solvent-based approach, Domenici C. et al. also demonstrated that the incorporation of 30 wt-% of PMMA totally promotes the β-phase to the detriment of α-phase[31]. Leonard et al. also specifically observed that the PVDF crystallization is sensitive to the cooling rate applied from the melt state[32] and, according to these observations, a recent investigation was performed by our group using Flash DSC to identify the impact of the cooling rate from the melt state on the crystallization of neat PVDF and PVDF/PMMA blends[33,36]. These thermal analyses under fast cooling rates allowed to obtain quantitative information on the crystallization temperature of non-polar and polar phases over large range of cooling rates (-10 to -4000 °C/s). A high cooling rate plays an essential role on the appearance of the PVDF β-phase with a clear α-to-β crystal transition. The polar β-phase starts to crystallize for cooling rates higher than 400 °C/s for neat PVDF with an exclusive/full crystallization for cooling rates after 1000 – 2000 °C/s. PMMA significantly shifted the α-to-β transition to lower cooling rates with the polar β-phase crystallization starting at cooling rates close to 50-100 °C/s with 10 wt-% PMMA[33]. These results allowed to obtain a clear crystal phase diagram of α-to-β crystal transition (with α+β mixed crystallization regime) as a function of PMMA and cooling rate. These diagram also revealed the ability of PVDF/PMMA blends to promote the polar β-phase with standard processing tools used in the plastic industry and the extrusion-calendering processing of PVDF/PMMA blends with an intense cooling rate applied during film calendering turned out to be an efficient way to produce thin films containing high amounts of β-crystals with only 5 wt-% of PMMA[33]. This process coupled to the addition of PMMA consequently represents an effective approach to reach

electroactive properties for PVDF using a cost-competitive melt-state technique without any solvent required and without supplementary pre/post treatments.

In terms of piezoelectric/ferroelectric properties, such PVDF/PMMA blends have not been deeply investigated and the data from literature shows some discrepancies. Some authors reported the reduced piezoelectric/ferroelectric properties such as remanent polarization P_r and coercive field E_c with the incorporation of PMMA into PVDF[15,27]. Recent results from our group also demonstrated a remanent polarization close to 2.4 μC/cm² with 10 wt-% PMMA[33] at a poling field of 2000 kV/cm, much weaker than the value for stretched PVDF film (close to 5.5 μC/cm² at the same poling field[37]). PVDF crystal size effects could explain the reduction of the electroactive properties for PVDF/PMMA blends[38]. Other research groups investigated the role of amorphous/crystalline interphase in miscible PVDF/PMMA and showed a significant importance of this interphase on the dielectric behavior[19]. Stingelin et al. observed a complex ferroelectric behavior for PVDF/PMMA blends with a typical hysteresis loop related to a capacitance phenomenon in the case of PVDF/PMMA blends with 10 wt-% PMMA[27]. The capacitance phenomenon seems to indicate charge trapping during high-voltage poling. This phenomenon could be linked to the crystal-amorphous interphase and the intercrystalline amorphous region with a swelling effect induced by PMMA on the crystalline component[39]. These investigations clearly indicate complex dielectric effects in PVDF/PMMA blends and the effect of PMMA on ferroelectric/piezoelectric properties of PVDF requires a careful examination to optimize PVDF/PMMA blends, in particular for melt-extruded films with a high amount of β-phase.

The inner structure and resultant physical properties of PVDF/PMMA blends could be modify and tailor using functional PMMA-based additives. Such approaches were previously depicted by several research group with blocky-like copolymers based on methyl methacrylate (MMA) and

functional comonomers. Wang P. et al. reported the use of 1-vinyl-3-ethyl imidazolium bromine ionic liquids (IL) to prepare P(MMA-IL) which is incorporated into PVDF by solution mixing[40]. The imidazolium cation of the IL through its ion-dipolar interactions with -CF_2 groups of PVDF can promote the PVDF β-phase and improve electric charge transfer in both amorphous and interphase regions. Poly(ethylene oxide)-*block*-poly(methyl methacrylate) (PEO-*b*-PMMA) or poly(methyl methacrylate-*co*-poly(ethylene glycol) methacrylate) (PMMA-*co*-PEGMA) mixed with PVDF could also exhibit higher ionic conductivity at room temperature ($2.8 – 3.10^{-3}$ S/m in comparison to $0.5.10^{-3}$ S/m for the neat PVDF)[41,42]. Other blocky-like copolymers were studied to modify the electroactive PVDF properties such as zwitterionic blocks or poly(2-vinyl pyridine) but no piezoelectric/ferroelectric were shown[43,44]. It could also be noticed that peculiar relaxor/antiferroelectric-like were also depicted for PVDF-based materials blends with several copolymers (P(VDF-TrFE-CTFE)-*g*-PMMA, P(VDF-TrFE-CTFE)-*g*-PEMA, P(VDF-TrFE-CTFE)-*g*-PS) with an interesting perspectives as energy storage/supercapacitors[45–47]. In this context, the use of functional PMMA-based copolymers clearly represents an interesting approach to develop new PVDF/PMMA materials with enhanced physical properties and a specific examination is mandatory.

In this respect, the following study is dedicated to the development of new PVDF materials using functional PMMA-based additives for the development of cost-effective advanced materials made by standard tools of the plastic industry. The incorporation of PMMA into PVDF combined with an extrusion-calendering technology was previously found of high interest for this purpose. An optimal PMMA content was detected close to 5 wt-% but only modest ferroelectric properties were reached in agreement with a moderate β-crystal production during the extrusion-calendering process. In this context, we here propose to investigate the use of poly(methyl methacrylate-*co*-

methacrylic acid) copolymers (PMMA-*co*-MAA, hereafter called PMMA-MAA) containing ionizable groups via the methacrylic acid moiety. This copolymer is theoretically able to modify the miscibility with PVDF, boost the β-crystal production during extrusion-calendering and increase resultant ferro/piezoelectric performances. Such additives containing ionizable moieties could also modify the dielectric behavior of the blends with potential intense effects on ferro/piezoelectric properties. Consequently, this study particularly emphasizes on how the use of PMMA-MAA copolymers alter the PVDF/PMMA miscibility, the related β-phase crystallization during melt-state processing and subsequent ferro/piezoelectric properties. Based on a previous investigation by our group, a preliminar study was conducted by Flash DSC to identify the impact of PMMA-MAA on the β-phase crystallization. A transposition to extrusion-calendered films was then performed followed by WAXS/FTIR characterizations to detect and quantify crystalline phases. A particular interest was subsequently carried on the ferroelectric/piezoelectric performances of as-produced PVDF/PMMA-MAA blends. The occurrence of crystal transformations during high-voltage poling and the impact of the high-voltage poling temperature on ferroelectric performances of PVDF/PMMA blends are finally discussed.

2. Experimental section

2.1.Materials

Poly(vinylidene difluoride) was kindly supplied by Arkema, France (hereafter called PVDF, grade Kynar® 720, M_w 200 000 g.mol^{-1}, MVR 10 cm^3/10min @ 230°C, 5kg). Poly(methyl methacrylate) was supplied by Evonik, Germany (hereafter called PMMA, grade 8N, M_w 97 000 g.mol^{-1}, MVR 3 cm^3/10min @ 230°C – 3.8kg). Poly(methyl methacrylate-*co*-methacrylic acid) (hearafter called PMMA-MAA, M_w 34500 g.mol^{-1}, MAA content 1.6 mol-%) was supplied by

Sigma-Aldrich Chemistry. Throughout this contribution, all percentages are given as weight percentage (wt-%).

2.2.Processing of PVDF/PMMA and PVDF/PMMA-MAA blends

PVDF-based blends with PMMA-based additives were melt-processed by a film extrusion-calendering process as described in a previous article by our group[33]. In a first step, PVDF and PMMA (or PMMA-MAA) were melt-blended in a co-rotating twin-screw extruder (Haake Rheomex PTW 16 OS, ThermoScientific, Germany) with a screw diameter of 16 mm for a L/D ratio of 40. Predetermined weight ratio of PVDF and PMMA (or PMMA-MAA) pellets were dry-blended, extruded (screw speed between 150 – 200 rpm, mass flow rate between 1– 1.2 kg/h) and pelletized. Extrusion temperatures were set to 210 °C (except for the temperature of extrusion die set at 170 °C). As-produced blends were reprocessed by film extrusion-calendering with a Haake single-screw extruder with a L/D ratio equal to 16, a temperature profile of 170 – 210 – 210 – 230 °C (from the hopper to the die) and a screw speed of 60 rpm. A specific slit die for film extrusion (width 150 mm, thickness 800 μm) was used and the film extrudate was subsequently calendered to obtain 20 – 40 μm thick films (accurately measured using a Köfer mechanical comparator, resolution +/- 1 μm). The calendering system is equipped with a cooling system using cold water (10 °C) within the cylinders (estimated cooling rate ± 200 °C/s according to the literature)[33].

2.3.Characterizations

2.3.1. Attenuated Total Reflectance Fourier Transform InfraRed spectroscopy (ATR-FTIR)

As-produced thin films were analyzed by Attenuated Total Reflectance Fourier Transform InfraRed spectroscopy (ATR-FTIR) using a BIO-RAD Excalibur spectrometer equipped with an ATR Harrick Split Pea™ apparatus from SAFIR Cie. Spectra were recorded using a spectral width

ranging from 700 to 1400 cm^{-1} with a resolution of 4 cm^{-1} and an accumulation of 64 scans. Peak areas at selected wavenumbers were determined using local baselines. ATR-FTIR spectra were systematically normalized to a reference peak (872 cm^{-1}) to dismiss the impact of film thickness variations on IR absorbance.

PVDF α- and β-crystallinities in as-produced films by extrusion-calendering were evaluated by ATR-FTIR according to previous studies by Gregorio et al.[2,48]. Relationships between peak intensity and crystal concentration were adapted for ATR-FTIR. The content in α-crystals was first calculated from **Relation 1** using baseline-corrected absorbance at 760 cm^{-1} (A_{760}) and at 870 cm^{-1} (A_{870}). The proportionality constant $K_{760/840}$ was set to 1.4 using a reference PVDF sample fully crystallized into the α-phase ($X_{c-\alpha}$ 55 % determined by DSC with an infinite ΔH_α of 104.5 J/g[2,36,39], $A_{760/A870} \approx 0.8$ determined by ATR-FTIR). The content in β-crystals was calculated from **Relation 2** using the baseline-corrected absorbance at 840 cm^{-1} (A_{840}). Since no reference PVDF sample fully crystallized into β-phase is available (with unknown value for infinite ΔH_β), the proportionality constant $K_{760/840}$ was obtained by **Relation 3** based on previous studies by Gregorio et al.[2,48].

$$X_{c-\alpha} = K_{760/870}^{ATR-FTIR} \frac{A_{760}}{A_{870}} \quad \textbf{(1)}$$

$$X_{c-\beta} = K_{840/870}^{ATR-FTIR} \frac{A_{840}}{A_{870}} \quad \textbf{(2)}$$

$$K_{840/870}^{ATR-FTIR} = 1.26\, K_{760/870}^{ATR-FTIR} \quad \textbf{(3)}$$

2.3.2. 2D-Small and Wide Angle X-ray Scattering (2D-SAXS & 2D-WAXS)

As-produced thin films were analyzed by both Small and Wide Angle X-ray Scattering (SAXS & WAXS). Analyses were carried out at room temperature in transmission mode on a Xeuss apparatus (Xenocs, France). The CuKα radiation (λ=1.542 Å) was used. The sample to detector

distances (calibrated using silver behenate) were set to approx. 10 cm and 120 cm for WAXS and SAXS respectively. The 2D patterns were recorded using a Pilatus detector (Dectris). Standard corrections (background, dark, etc...) were applied to the patterns before analyses and integrated intensity profiles were computed using the Foxtrot software.

2.3.3. DSC and Flash DSC (FDSC)

Flash DSC (FDSC) experiments were carried out on a Mettler-Toledo Flash DSC 1 via a specific protocol to observe the crystallization behavior of as-produced PVDF/PMMA-based blends at different cooling rates. The detailed procedure could be found in our previous article on this topic[33]. Briefly, samples of about 35 – 100 ng were placed on the active area of the circular 500 μm-diameter sensor using an optical microscope. The FDSC method for crystallization analyses is the following: heating at 1000°C/s to 210 °C, isotherm at 210°C during 10 s, cooling at controlled cooling rates between -10°C/s and -4000°C/s to -80°C, isotherm at -80°C during 10 s, heating at 5000°C/s to 210 °C. Crystallization temperatures (T_c) were determined at the maximum of the exothermic peak observed during the cooling scan. For sake of clarity, cooling curves were normalized by the cooling rate.

2.3.4. Ferroelectric and piezoelectric properties

All electrical characterizations were carried out on metallized thin films with Ag electrodes deposited by vacuum sputtering (electrode area 7 mm²). Ferroelectric-type (P-E)/(I-E) loops were characterized in a dielectric liquid bath (FC40, 3MTM FluorinertTM) by a current integration method[49–51]. Low-frequency (0.1Hz) and high-voltage sine waves were applied by the combination of a synthesizer/function generator (HP3325B, Hewlett Packard Inc., Palo Alto, CA) and a high-voltage amplifier (Trek Model 10/40A, Medina, NY). Surface charges were measured with a homemade charge-to-voltage converter. Ferroelectric-type (P-E)/(I-E) loops are presented after

compensation, *i.e.* after subtracting linear polarization and conduction contributions from the current response, by assuming a resistance and a capacitance in a parallel model. For each measurement (*i.e.* for each applied electric field), several consecutive high-voltage cycles (3 to 5 cycles) were performed to ensure a stable switching behavior. The piezoelectric coefficient d_{33} was then obtained with a Berlincourt piezometer (Channel Products Inc. Chesterland, OH, mechanical stress condition of 100 Hz and 0.25 N). High-voltage poling was accomplished under the maximum field attained during (P-E)/(I-E) characterizations (typically 1500 kV/cm) by removing the field just before completing the loop. The Ag electrodes were eventually removed for specific physico-chemical analysis using cotton tips impregnated with diluted hydrochloric acid followed by immediate rising with distilled water.

2.3.5. Visual and optical inspections

Optical properties of as-produced thin films (transmittance, haze and clarity) were investigated and quantified using a specific test bench from BKY Gardner (Germany, HazeGrad Plus). As-produced thin films were also investigated by optical microscopy in reflection mode using Leica DM 2500M microscope (magnification x20) to reveal blend microstructures.

3. Results and discussions

3.1. PVDF/PMMA-MAA miscibility and β-phase crystallization analyzed by FDSC

To get precise information regarding the PVDF/PMMA-MAA miscibility and the use of PMMA-MAA as a β-phase promoter for PVDF, a preliminar study was conducted by Flash DSC on selected compositions before a transposition to extrusion-calendered films. PVDF blends with 5 – 10 wt-% PMMA-MAA obtained using a melt-state twin-screw extrusion process were submitted to FDSC analysis and crystallization exotherms from the melt state were recorded at

various cooling rates, ranging from 10 to 2000°C/s (**Figure 1AB**). A particular attention was paid to the α-to-β crystal transition with respect to the cooling rate (**Figure 1C**) and the apparent β-phase fraction as a function of the cooling rate was extracted from relative crystallization enthalpies. Comparisons with PVDF/PMMA blends were performed and crystallization temperatures T_c were also extracted for α-/β-crystallizations (**Figure SI1**) to get a better view of PVDF/PMMA-MAA miscibility.

PVDF/PMMA-MAA blends with 5 wt-% PMMA-MAA exhibit a single exotherm for low cooling rates (< 100 °C/s) with crystallization temperatures in the range of 110 – 70°C. A second distinct exotherm at lower crystallization temperatures in the range 60 – 20°C appears at higher cooling rates and becomes predominant at elevated cooling rates. Based on previous studies by our group[33], the first exotherm is ascribed the PVDF α-crystallization and the second low-temperature exotherm to the PVDF β-crystallization. Thus the PMMA-MAA copolymer also prone the α-to-β crystal transition, similarly to neat PVDF and PVDF/PMMA blends (at 5 wt-% PMMA). The α-to-β crystal transition occurs between 100 and 600°C/s, such values being much lower than neat PVDF with β-phase crystallization starting around 400°C/s[33]. The evolution of the crystallization temperatures as a function of the cooling rate (**Figure SI1**) also reveals a significant shift to lower T_c for both α- and β-crystallization in PVDF/PMMA-MAA compared to neat PVDF attesting for a good PVDF/PMMA-MAA miscibility. A comparison could be also performed with the corresponding PVDF/PMMA blend with 5 wt-% PMMA. The efficiency of PMMA-MAA for β-phase production seems to be slightly better than PMMA with a tiny reduction of the crystallization temperatures and shift of α-to-β crystal transition (transition in the range 120 – 700°C/s for PVDF/PMMA blend with 5 wt-% PMMA) (**Figure SI1**).

For PVDF/PMMA-MAA blends with 10 wt-% PMMA-MAA, the α-to-β crystal transition is clearly shifted to lower cooling rates in a similar way than PVDF/PMMA blends[33]. The β-phase could appear for cooling rates as low as 60°C/s and slightly better performances are again attested for PVDF/PMMA-MAA containing 10 wt-% PMMA-MAA compared to PMMA (in particular at elevated cooling rates). Significant reductions of the α-/β-crystallization temperatures are also detected (**Figure SI1**). In this context, FDSC consequently suggests a good miscibility of PMMA-MAA with PVDF in the concentration range 5 – 10 wt-% PMMA-MAA with slight positive influence of PMMA-MAA compared to PMMA for the β-phase production during cooling from the melt state (in particular at representative cooling rate of the extrusion-calendering process). These effects could be attributed to enhanced PVDF/PMMA-MAA interactions inducing higher miscibility with PVDF, in agreement with findings by Landis et al. on PVDF crystallization in the presence of tiny amounts of PMMA-MAA[52].

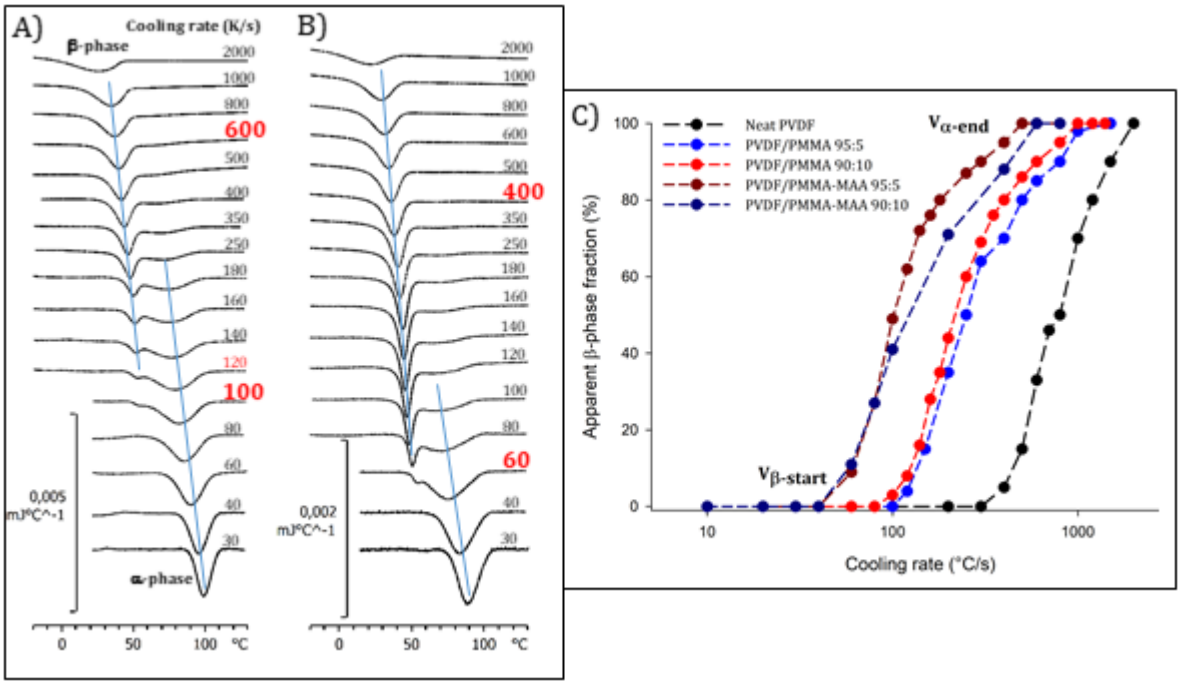

Figure 1. FDSC cooling scans at various cooling rates obtained for PVDF/PMMA-MAA blends with 5 wt-% PMMA-MMA (A) and 10 wt-% PMMA-MAA (B) (critical cooling rates for the apperance of the β-phase and disapperance of the α-phase are marked in red. Apparent β-phase fraction (C) as a function of the cooling rate for neat PVDF (black), PVDF/PMMA with 5 wt-% PMMA (blue), PVDF/PMMA with 10 wt-% PMMA (dark blue), PVDF/PMMA-MAA blends with 5 wt-% PMMA-MAA (red) and PVDF/PMMA-MAA blends with 10 wt-% PMMA-MAA (dark red). Datas for neat PVDF and PVDF/PMMA with 5 – 10 wt-% PMMA are taken from previous measurments[33].

3.2. β-phase crystallization in PVDF/PMMA-MAA films produced by extrusion-calendering

Taking into account FDSC results, thin films of PVDF/PMMA-MAA (thickness range of 25 – 35 μm) were produced by melt-state extrusion-calendering process that provide intense cooling rates (± 200°C/s depending on film thickness and materials)[33]. Thin films were then characterized by ATR-FTIR and WAXS to observe the evolution of the PVDF crystalline phases with the incorporation of 5 and 10 wt-% PMMA-MAA. ATR-FTIR is an accurate characterization technique for PVDF crystalline phases that potentially enables qualitative and quantitative measurements for the β-phase (characteristic absorption peak at 840 cm^{-1}) and for the α-phase (characteristic absorption peak at 766, 795 and 855 cm^{-1})[2,48,53]. To discriminate the polar phases and confirm ATR-FTIR analyses, WAXS characterizations were used to identify the crystalline lattices[2] related to β- and α-phase at a 2θ angle of 20.8° and 18.3, 19.9, 26.6°, respectively. ATR-FTIR and WAXS analyses are also of good interests to detect the PVDF γ-phase (characteristic absorption peaks at 776, 812 and 1234 cm^{-1})[2,48,53]. **Figure 2** displays ATR-FTIR and WAXS characterizations of PVDF, PVDF/PMMA and PVDF/PMMA-MAA blends. First, the neat PVDF

film displays mostly the characteristic peaks of the non-polar α-phase (765, 795 and 855 cm^{-1}). A slight β-phase crystallization is observed (840 cm^{-1}) due to high cooling rates. WAXS analysis for neat PVDF films also shows the apparition of a small shoulder at 20.5°, which confirm the slight amount of β-phase.

For PVDF/PMMA and PVDF/PMMA-MAA blends with 5 wt-% PMMA-based additives, a clear modification of the PVDF crystallization is observed. ATR-FTIR allows confirming the high positive influence of PMMA-MAA on the β-phase crystallization during film extrusion-calendering compared to PMMA. Indeed, the absorption peak related to the β-phase at 840 cm^{-1} clearly displays a higher intensity for the PVDF/PMMA-MAA blend than the corresponding PVDF/PMMA blends. In the opposite, α-phase absorption peaks are reduced. WAXS analysis confirms the effect of PMMA-MAA on β-phase crystallization with a clear β-phase pattern (20.3°) and a quasi-disappearance of α-phase diffraction peak at 2θ angle close to 26.6°. To complete these analysis, it could be mentioned that (i) the γ-phase is not detected (absence of any absorption peaks at 776, 812 and 1234 cm^{-1}, **Figure SI2**) thus confirming the α-to-β crystal transition in PVDF/PMMA blends processed by extrusion-calendering and (ii) unoriented α-/β-crystals are detected by 2D-WAXS (**Figure 2**) indicating that α-/β-crystallization seems to proceed from a quasi-isotropic melt state. In this context, PMMA-MAA acts as a powerful β-phase promoter for PVDF using a melt-state extrusion-calendering process, such result being partly consistent with previous FDSC experiments. Actually, it could be stated out that the efficiency of PMMA-MAA seems to be significantly higher in dynamic conditions (*i.e.* after shearing treatments by extrusion) than in static conditions (*i.e.* during FDSC analysis).

Similar analyses were performed for PVDF-based blends with 10 wt-% PMMA-based additives (**Figure 2**) and ATR-FTIR/WAXS experiments clearly show an opposite evolution in terms of

PVDF crystallization. First, the incorporation of 10 wt-% PMMA favors β-crystallization as observed by the increase of β-peak intensity and the typical WAXS patterns of β-phase, in accordance with previous studies[33]. On the contrary, the incorporation of 10 wt-% of PMMA-MAA drastically inhibited the β-phase crystallization. A predominant α-phase and a very low β-phase content is detected for this particular blend, such result being confirmed by WAXS analysis. Deeper investigations were performed to detect the miscibility extent after the extrusion process of this particular blend using visual/optical inspections and SAXS analysis (**Figure SI3**). The PVDF/PMMA-MAA blend with 10 wt-% PMMA-MAA displays an opaque appearance that was quantified by optical measurements with a higher haze value (21% compared to 4 – 5% for other blends) coupled to a lower clarity value (77% compared to 99 – 97% for other blends). This effect is linked the heterogeneous/texturized microstructure of this particular blend and suggests a reduced miscibility extent. The peculiar 2D-SAXS pattern also confirmed the presence of nanoscale oriented/elongated domains. All these elements coupled to the significant discrepancy with previous FDSC analysis clearly suggest that PVDF/PMMA-MAA blends are unstable in dynamic/shearing conditions. This demixing phenomenon in shearing conditions induces complex effects on PVDF crystallization (enhanced β-phase crystallization at 5 wt-% PMMA-MAA and inhibited β-phase crystallization at 10 wt-% PMMA-MAA). Such conclusions could be agreement with previous conclusions from Landis et al. demonstrating that an elevated quantity of MAA moieties could have a negative effect on the resulting compatibility[52]. Finally, differences in molecular weight between PMMA-MAA (37 500 g/mol) and PMMA (97 000 g/mol) with large subsequent differences in melt viscosity/terminal relaxation times could explain this demixing phenomena in intense shear/elongation flows. Detailled investigations are required by the future to reproduce this phenomenon in controlled shear/elongation environment to stabilize/control the

microstructure and the miscibility extent of PVDF/PMMA-MAA blends (in particular at elevated PMMA-MAA content.

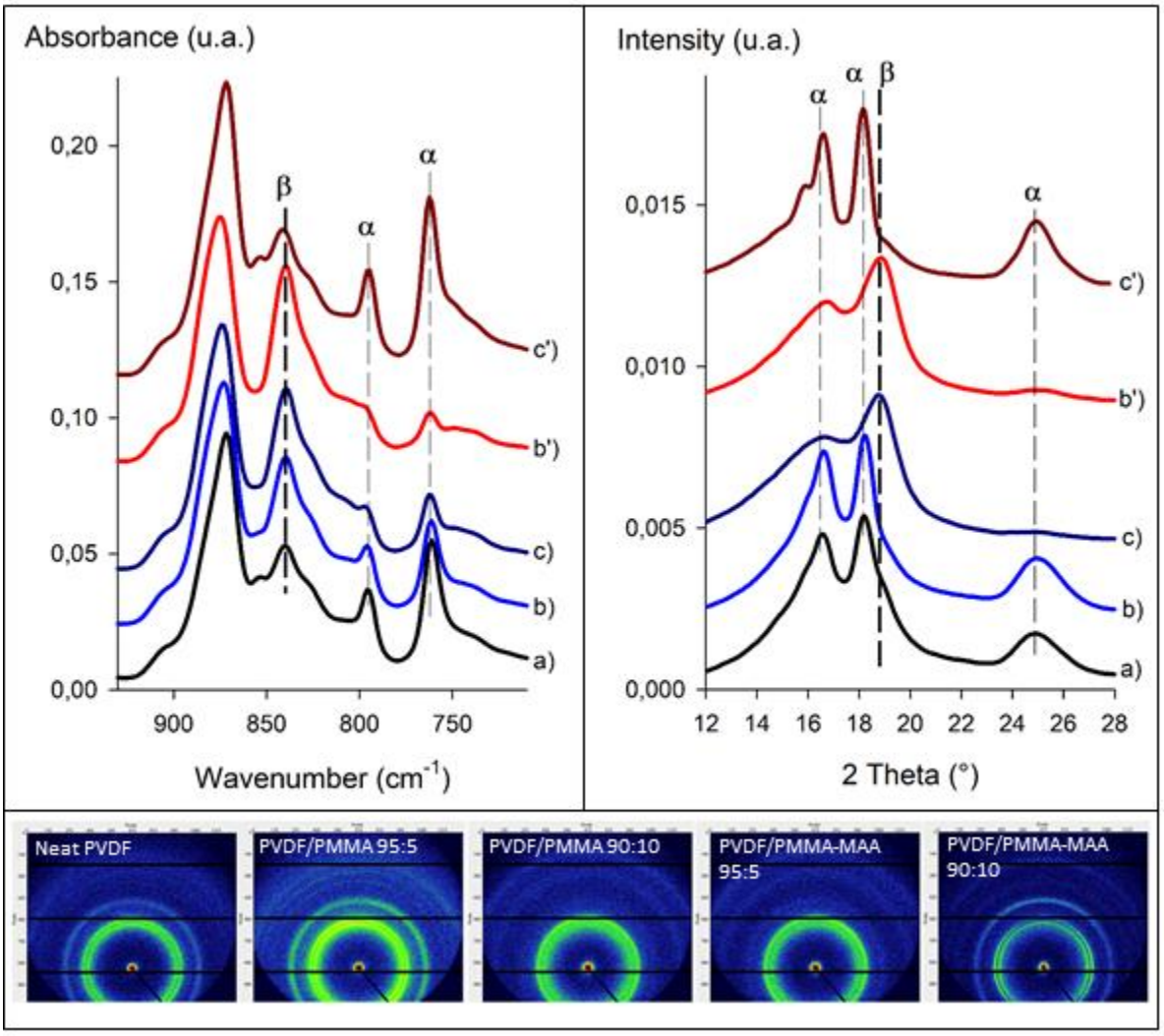

Figure 2. ATR-FTIR (left) and WAXS (right) spectra of PVDF/PMMA and PVDF/PMMA-MAA blends processed into films by extrusion-calendering. Neat PVDF (a – black), PVDF/PMMA 95:5 (b – blue), PVDF/PMMA-MAA 95:5 (c – dark blue), PVDF/PMMA 90:10 (b' – red) and PVDF/PMMA-MAA 90:10 (c' – dark red). Corresponding 2D-WAXS spectrum are displayed in the lower box.

Quantitative information about PVDF α- and β-crystallinities in as-produced thin films were obtained by ATR-FTIR and the evolution of PVDF crystals contents with the amount of PMMA or PMMA-MAA is tabulated in **Table 1**. Neat PVDF films display a total crystallinity of ± 56 % (α+β crystals) with approx. 45 – 50 % of α-crystals and 5 – 10 % of β-crystals. The evolution of PVDF total crystallinity as a function of PMMA content displays a continuous decrease in agreement with the PVDF/PMMA miscibility[28,33]. Besides, the content in α-crystals clearly and quickly drops with the amount of PMMA with a total disappearance for 20 wt-%, in agreement with the α-to-β crystal transition with the incorporation of PMMA. The amount of β-phase reaches the entire crystallinity at this peculiar PMMA content. Similar calculations were performed for PVDF/PMMA-MAA with an interesting β-phase content of 35 % (total crystallinity 45 %, β-phase fraction 78 %, **Table 1**) for only 5 wt-% PMMA-MAA. The high reduction of the β-phase content in PVDF/PMMA-MAA blends incorporating high PMMA-MAA loadings (10 wt-%) is here confirmed (total crystallinity 52 %, β-phase content 8%,). To conclude, compared to the use of PMMA, PMMA-MAA clearly enhances the production of PVDF β-crystals from the melt state using an extrusion-calendering process with elevated cooling rates applied to thin films. However, the amount of PMMA-MMA should be carefully controlled and limited to 5 wt-% to avoid demixing phenomenan in dynamic/shearing conditions during extrusion at higher PMMA-MAA loadings.

Table 1: PVDF crystalline phase contents (α-crystals, β-crystals and total α+β-crystals) in PVDF/PMMA and PVDF/PMMA-MAA blends processed into films produced by extrusion-calendering (evaluation by ATR-FTIR, standard deviation into brackets).

	$X_{c\text{-}\alpha\text{-crystals}}$ (%)	$X_{c\text{-}\beta\text{-crystals}}$ (%)	$X_{c\text{-}\alpha+\beta\text{-crystals}}$ (%)

Neat PVDF	48 (4)	8 (4)	56 (1)
PVDF/PMMA 95:5	33 (4)	19 (4)	52 (1)
PVDF/PMMA 90:10	16 (2)	27 (2)	43 (1)
PVDF/PMMA 80:20	1 (1)	31 (1)	32 (1)
PVDF/PMMA-MAA 95:5	10 (1)	35 (1)	45 (1)
PVDF/PMMA-MAA 90:10	43 (2)	8 (1)	52 (1)

3.3. Ferroelectric properties of PVDF/PMMA-MAA films produced by extrusion-calendering

Previous crystallinity characterizations enable to select interesting materials for subsequent ferroelectric/piezoelectric studies. Actually, the PVDF/PMMA-MAA blend displays an interesting β-phase content of 35 % (total crystallinity 45 %, β-phase fraction 78 %) with only 5 wt-% PMMA-MAA and thus represents an interesting candidate for ferro/piezoelectric applications. To analyze ferroelectric properties/performances under poling at high AC electric fields and obtain correlations to PVDF crystal structures, (P-E)/(I-E) hysteresis loops were recorded for as-produced thin films by extrusion-calendering. These loops allow the identification/quantification of the ferroelectric switching behavior with the ability to perform an efficient poling under AC electric fields for further piezoelectric testing. The remanent polarization P_r (permanent dipole orientation/polarization after voltage removal) is extracted from the (P-E) loops along with a ferroelectric quality factor (*i.e.* ratio between remanent polarization and saturation polarization, P_r/P_{sat} with P_{sat} the maximum dipole orientation/polarization achieved for each applied voltage). (I-E) loops reveal charge displacements inside the analyzed materials with the estimation of the coercive field E_c (electric field required for dipole switching). **Figure 3** displays (P-E) loops from neat PVDF, PVDF/PMMA and PVDF/PMMA-MAA films at various electric fields ranging from

1000 to 1500 kV/cm. Corresponding (I-E) loops could be found in the Supporting Info section (**Figure SI4**). Quantitative values for P_r and E_c at the maximal electric field of 1500 kV/cm are tabulated in **Table 2** and **Figure 4** gathers the evolution of P_r and E_c values as a function of the electric field.

With an applied electric field of 1500 kV/cm, neat PVDF displays ferroelectric-type behavior (**Figure 3A**) with P_r close to 2.2 μC/cm², E_c close to 825 kV/cm and a quality factor of 0.78 (**Table 2**). These values are lower than those obtained by Mackey et al.[37] on stretched PVDF poled at the same electric field (P_r close to 5.5 μC/cm²). Discrepancies are also observed with previously-reported results in the corresponding literatures[8,33,37,54,55], partly attributed to (i) the impact of the extrusion processing method with high cooling rates to produce polar β-crystals and (ii) compensation procedures to remove non-switching charges during (P-E)/(I-E) measurements. It should be noted that neat PVDF showed a hard ferroelectric switching behavior for electric fields below 1200 kV/cm with back-switching phenomena (dipole rotation without full switch/fixation)[56]. It is also clear from (P-E) loops that neat PVDF is far from polarization saturation and thus higher electric fields than 1500 kV/cm would be required. (I-E) curves also indicate that the switching is not homogeneous throughout the material with a broad distribution of coercive fields typically observed with poorly-poled materials in the pre-switching regime (**Figure SI4**).

Incorporating 5 wt-% of PMMA into PVDF clearly improves ferroelectric properties (**Figure 3B**) with P_r up to 4.3 μC/cm², E_c close to 770 kV/cm and a quality factor of 0.88 at the maximal electric field of 1500 kV/cm (**Table 2**). These values still remain below those reported for stretched PVDF poled at the same electric field but square (P-E) loops approaching polarization saturation are obtained and (I-E) curves indicate a more homogenous switching behavior with a narrower

distribution of coercive fields (**Figure SI4**). However, higher PMMA content (10 wt-%) clearly reduces ferroelectric properties with a total transformation into quasi-linear dielectric-like behavior at 20 wt-% PMMA (**Figure 3C-D** and **Table 2**), despite a continuous increase of polar β-phase content with higher amounts of PMMA (β-phase content up to 31% at 20 wt-% PMMA, β-phase fraction close to 100% **Table 1**). This apparent ferroelectric vanishing could be related with a strong clamping of β-phase dipoles that hinders their effective polarization. This is a well-known phenomenon in ferroelectric materials usually associated to the presence of dipolar defects that interacts with the spontaneous polarization.

The addition of 5 wt-% of PMMA-MAA copolymer into PVDF further improved ferroelectric properties in comparison with corresponding PVDF/PMMA blend (**Figure 3E**). P_r close to 5 μC/cm², E_c of 740 kV/cm and an excellent quality factor of 0.85 are obtained at the maximal electric field of 1500 kV/cm (**Table 2**). Again, square (P-E) loops indicate that polarization saturation is being approached with an homogeneous switching behavior (**Figure SI14**). Coercive fields are interestingly lower in PVDF/PMMA-MAA (with higher remanent polarization) and these effects indicate that the PMMA-MAA copolymer not only modifies the dipole density (related to β-phase content) but also their own switching dynamics. Higher incorporation of PMMA-MAA again results in reduced ferroelectric properties but, in this case, this effect is in agreement with the significant decrease of β-phase content for 10 wt-% PMMA-MAA related to its immiscibility with PVDF (**Figure 3F** and **Table 2**).

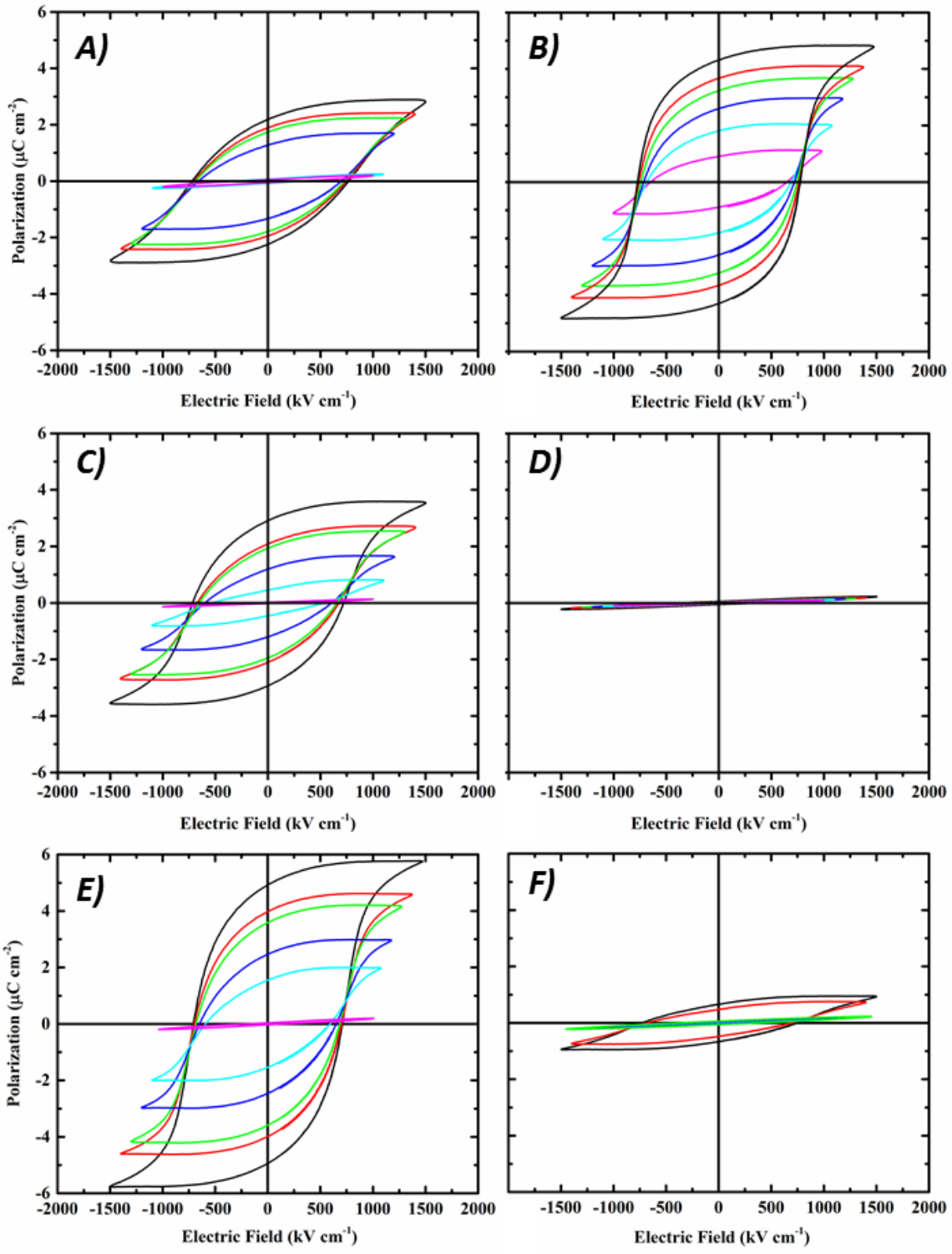

Figure 3. (P-E) hysteresis loops under increasing AC electric fields recorded at room temperature for PVDF/PMMA and PVDF/PMMA-MAA blends processed into films by extrusion-calendering.

Neat PVDF (A), PVDF/PMMA 95:5 (B), PVDF/PMMA 90:10 (C), PVDF/PMMA 80:20 (D), PVDF/PMMA-MAA 95:5 (E) and PVDF/PMMA-MAA 90:10 (F) (film thickness 25-35 μm).

Table 2. Remanent polarization, coercive field and ferroelectric quality factor for PVDF/PMMA and PVDF/PMMA-MAA blends processed into films by extrusion-calendering (AC electric field 1500 kV/cm, film thickness 25-35 μm) (n.m. not measured).

	P_r (μC/cm²)	E_c (kV/cm)	P_r/P_{sat}
Neat PVDF	2.2	825	0.78
PVDF/PMMA 95:5	4.3	770	0.88
PVDF/PMMA 90:10	3.0	760	0.79
PVDF/PMMA 80:20	0.1	n.m.	0.22
PVDF/PMMA-MAA 95:5	4.9	740	0.85
PVDF/PMMA-MAA 90:10	0.6	n.m.	n.m.

Figure 4 gives an interesting overview and allows concluding on the evolution of the ferroelectric properties with the applied electric field and the type/amount of PMMA additives. Neat PVDF needs elevated electric fields (> 1200 kV/cm) to induce a ferroelectric switching behavior with high E_c values. With the addition of 5 wt-% of PMMA or PMMA-MAA, ferroelectric-type behaviors appear at lower electric fields with significant increase of the remanent polarizations, lower coercive fields and higher ferroelectric quality factors. These results are an evidence that ferroelectric PVDF-based films could be produced by a melt-state extrusion-calendering process. The specific use of 5 wt-% PVDF/PMMA-MAA clearly enhanced ferroelectric properties. Such effect is primarily attributed to the improvement of the β-phase content induced by the extrusion-calendering processing (β-phase content up to 35%) but a contribution of ionic moieties to the dipole dynamics is also suspected. Our results also evidence

that the initial β-phase content does not seem to fully govern the final ferroelectric behavior and properties. Actually, neat PVDF with a low β-phase content displays small but interesting ferroelectric properties and no clear correlations are found between the remanent polarization achieved at elevated electric fields and the initial β-phase content. Other factors/parameters probably need to be considered for an in-depth understanding (like crystalline modifications at elevated electric fields, size of PVDF β-crystal and interfacial trapped charges[33]). However, a partial α-to-β crystal phase transformation under high electric fields is particularly anticipated in as-produced blends and this effect will be discussed within the next sections.

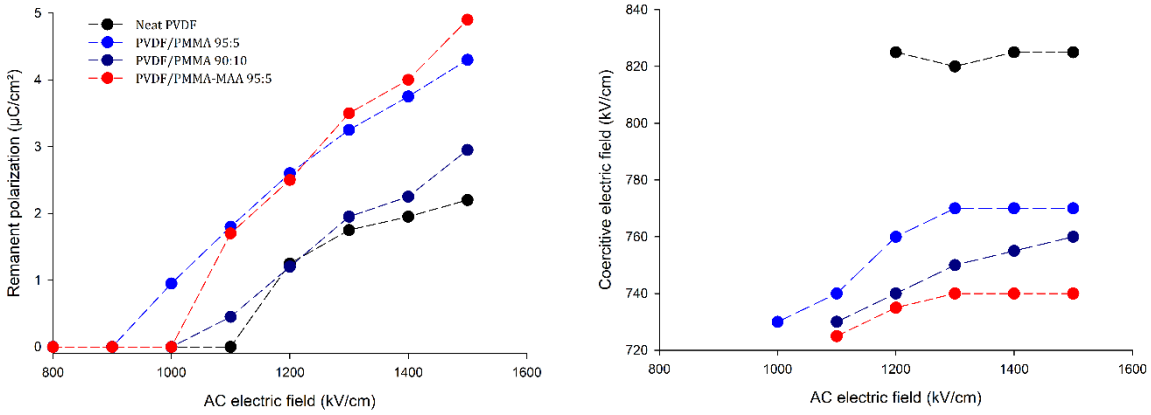

Figure 4. Evolution of the remanent polarization (left) and coercive electric field (right) with the applied AC electric field for neat PVDF (black), PVDF/PMMA 95:5 (blue), PVFD/PMMA 90:10 (dark blue) and PVDF/PMMA-MAA 95:5 (red) blends processed into films by extrusion-calendering (film thickness 25-35 μm).

3.4. Piezoelectric properties of PVDF/PMMA-MAA films produced by extrusion-calendering

Ferroelectric properties of PVDF-based materials are known to be correlated with their final piezoelectric properties and such properties are clearly of high interests for many emerging

applications. The corresponding literature indicates that ferroelectric/piezoelectric properties can be significantly affected by the presence of PMMA[15,27] and, taking into account previous results on ferroelectric properties, piezoelectric coefficients d_{33} were evaluated for as-produced PVDF/PMMA-MAA blends. The time stability of the piezoelectric coefficients d_{33} up to 2 weeks after the poling process was first addressed and quantitative values can be found in the Supporting Info section (**Table SI1**). The piezoelectric coefficient of neat PVDF after the poling procedure was found close to 7 pC/N (± 1 pC/N) decreasing to a stabilized value of 5 pC/N after a storage period of 1 week (**Table SI1**). Thus, a first remarkable result is that as-produced neat PVDF film displays a significant d_{33} value without stretching treatments[1–4]. PVDF/PMMA blends with 5, 10 and 20 wt-% of PMMA additives were subsequently subjected to the same poling procedure followed by piezoelectric measurements (**Table SI1**). As a general rule, the piezoelectric coefficient also decreases with storage time by approx. 1 – 2 pC/N after 1 week to reach a stabilized value. Such effects could be linked to residual electrostatic charges (electret effect) or/and charge losses inside the matrices due to relaxations. However, it could be stated out that stable piezoelectric properties are obtained for as-produced and as-poled PVDF/PMMA blends.

Figure 5 displays the evolution of the piezoelectric coefficient as a function of the PMMA or PMMA-MAA content. The evolution of the piezoelectric coefficient closely follows the trend observed on ferroelectric properties. Actually, a maximal d_{33} value is observed with 5 wt-% of PMMA or PMMA-MAA reaching a remarkable piezoelectric coefficient of approx. 11 pC/N. For higher PMMA or PMMA-MAA contents, piezoelectric properties drastically decrease. A close correlation is anticipated between piezoelectric coefficients (d_{33}) and remanent polarizations (P_r) and, as depicted in **Figure 5**, a linear relationship between d_{33} and P_r is nearly obtained with a slope of approx. 2. Such linear relationship is clearly in agreement with the recent models concerning

the piezoelectricity of PVDF, in particular with the electrostriction model[57] that yields a linear relationship with a slope close to 2.4. It could be noticed that the line does not pass through the origin with a residual piezoelectricity of approx. 1.5 pC/N as confirmed with PVDF/PMMA blends incorporating high PMMA contents up to 20 wt-%. These effects could be ascribed to trapped charges introduced during poling into as-produced PVDF/PMMA. As a conclusion, interesting piezoelectric properties are observed for PVDF blends with PMMA and PMMA-MAA processed into films by an extrusion-calendering technique. The impact of PMMA or PMMA-MAA on the piezoelectric properties is obvious with a maximal coefficient close to 11 pC/N for an optimum content of 5 wt-%. Nevertheless, in this case, no significant differences are noticed between PVDF/PMMA and PVDF/PMMA-MAA blends in term of piezoelectric activity. An interesting correlation with a linear relationship is obtained between piezoelectric and ferroelectric properties in PVDF/PMMA and PVDF/PMMA-MAA blends that points out the main importance of ferroelectric properties for further optimization.

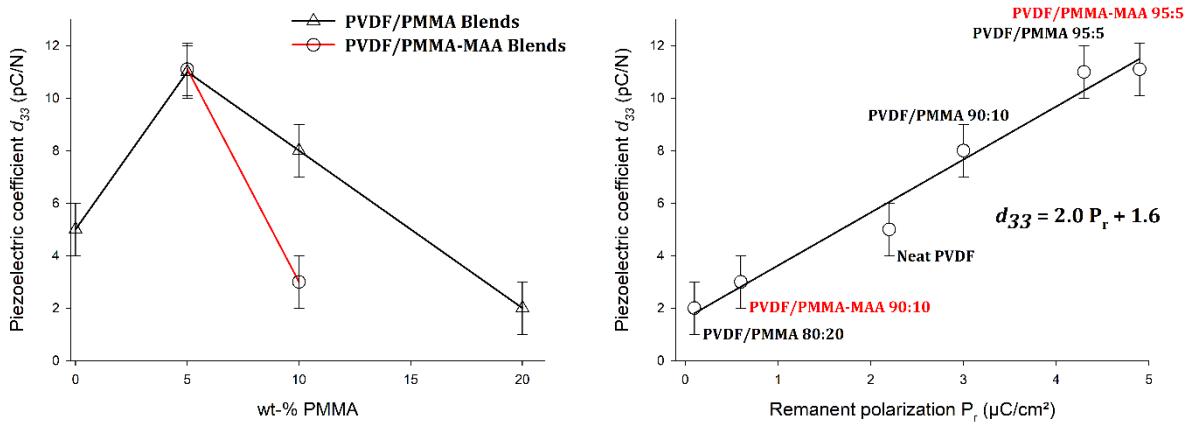

Figure 5. Evolution of the piezoelectric coefficient d_{33} with the amount of PMMA-based additives (left) and evolution of the piezoelectric coefficient d_{33} with the remanent polarization (right) for PVDF/PMMA and PVDF/PMMA-MAA blends processed into films by extrusion-calendering (high-voltage poling by AC electric field 1500 kV/cm, film thickness 25-35 µm).

3.5. Discussion on crystal transformations during high-voltage poling

As previously discussed, the initial β-phase content in as-produced PVDF-based films does not fully fit with ferroelectric properties and subsequent piezoelectric properties. Actually, neat PVDF films with a poor β-phase content develop significant ferro/piezoelectric properties but several PVDF/PMMA blends (in particular PVDF/PMMA blends with 10 – 20 wt% PMMA) with high β-phase contents display poor ferro/piezoelectric performances. An optimal content close to 5 wt-% is required to boost ferro/piezoelectric properties but, despite significant differences between PVDF/PMMA and PVDF/PMMA-MAA blends in terms of initial β-phase content, similar P_r and, in particular, d_{33} values results are obtained. One potential and interesting hypothesis lies in crystal transformations during high-voltage poling with a potential α-to-β crystal transformation at elevated electric fields[58,59]. Such modifications could drastically modify ferroelectric properties with repercussions on subsequent piezoelectric performances.

In this context, additional ATR-FTIR experiments were conducted on the PVDF-PMMA and PVDF/PMMA-MAA films processed by extrusion-calendering after the high-voltage poling process at 1500 kV/cm. ATR-FTIR spectra were compared with previous results before high-voltage poling (**Figure 6**) and quantitative parameters regarding crystal type/content are tabulated in **Table 3**. Based on ATR-FTIR spectra, crystalline modifications clearly occurred in neat PVDF films during high-voltage poling with a high increase in polar β-phase content from 8 % to 29 % (**Figure 6A** and **Table 3**). The α-phase content also clearly decreases in a similar magnitude, thus confirming an α-to-β crystal transformation during high-voltage poling for neat PVDF films and explaining the sizable ferroelectric switching behavior observed for this material.

Similar final crystal transformations are observed for PVDF/PMMA and PVDF/PMMA-MAA with 5 wt-% PMMA or PMMA-MAA with an increase of the β-phase peaks after poling together

with a decrease of α-phase peaks (**Figure 6BC**). The final amount of β-crystals reaches 38 – 39% for these blends (**Table 3**) in accordance with their enhanced ferroelectric properties. However, ferroelectric properties cannot be entirely correlated to the final amount of β-crystals after high-voltage poling, in particular for PVDF/PMMA blends with 20 wt-% PMMA (β-phase content close to 31%, β-phase fraction close to 100%). Actually, the α-to-β crystal transformation is known to occur via an intermediate polar α-phase, named α_p-phase, leading to a global α-to-α_p-to-β crystal transformation under high-voltage poling[58,59]. This pathway is here difficult to detect using ATR-FTIR but several abnormal trends are detected. On one hand, **Table 3** highlights variations in terms of total crystalline content before and after high-voltage poling with an apparent decrease in total crystallinity. Besides, the α-crystal peak located at 795 cm^{-1} corresponding to -CH_2 rocking vibrations[60] seems to follow different trends from the other α-crystal and this absorption peak does not decrease after high-voltage poling. In this context, a (partial) crystal transformation from the α-phase into α_p-phase during high-voltage poling seems consistent with our observations. Consequently, thanks to a α-to-α_p-to-β crystals transformation during poling, it can be assumed that a high initial β-phase content is not fully mandatory for enhanced ferro/piezoelectric performances. The non-polar α-phase could also contribute to ferroelectric properties of neat PVDF and PVDF/PMMA blends via a polar intermediate α_p-phase. The amount of these two crystalline phases after high poling voltage seems to control ferroelectric properties of PVDF/PMMA and PVDF/PMMA-MAA blends processed by extrusion-calendering. In-depth and challenging investigations are required in a near future to detect exact mechanisms behind α-to-α_p-to-β crystals transformation and the exact role of each crystalline phase (and *in fine* the role of PMMA and PMMA-MAA copolymers) on ferroelectric and piezoelectric properties of PVDF/PMMA and PVDF/PMMA-MAA blends.

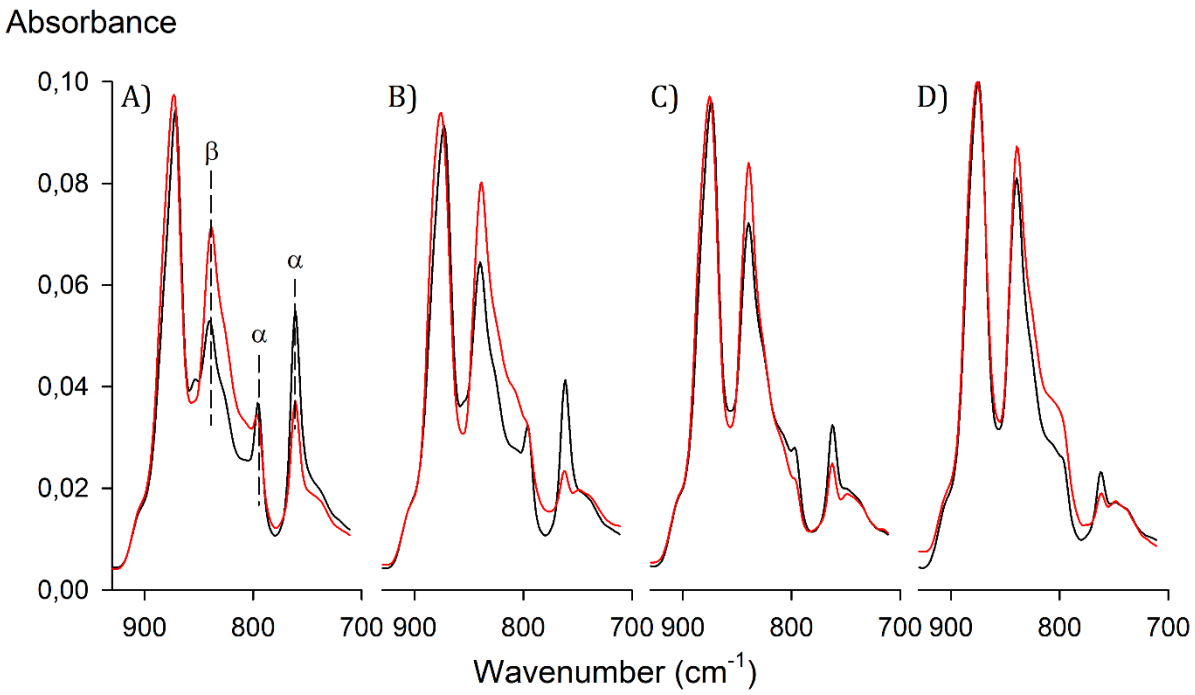

Figure 6. Impact of high-voltage poling on the ATR-FTIR spectra of neat PVDF (A), PVDF/PMMA 95:05 (B), PVDF/PMMA 90:10 (C) and PVDF/PMMA-MAA 95:05 (D) blends processed into films by extrusion-calendering (AC electric field 1500 kV/cm, film thickness 25-35 µm). Poled (red) and non poled (black).

Table 3. PVDF crystalline phase contents (α-crystals, β-crystals and α+β-crystals) in poled PVDF/PMMA and PVDF/PMMA-MAA blends processed into films by extrusion-calendering (evaluation by ATR-FTIR, AC electric field 1500 kV/cm, film thickness 25-35 µm, variations compared to unpoled films into brackets).

	$X_{c\text{-}\alpha\text{-crystals}}$ (%)	$X_{c\text{-}\beta\text{-crystals}}$ (%)	$X_{c\text{-}\alpha+\beta\text{-crystals}}$ (%)
Neat PVDF	20 (-28)	29 (+21)	49 (-7)
PVDF/PMMA 95:5	8 (-25)	38 (+19)	45 (-7)
PVDF/PMMA 90:10	6 (-10)	33 (+6)	40 (-3)

PVDF/PMMA 80:20	1 (0)	31 (0)	32 (0)
PVDF/PMMA-MAA 95:5	5 (-5)	39 (+4)	44 (-1)
PVDF/PMMA-MAA 90:10	44 (0)	10 (+1)	53 (+1)

3.6. High-voltage poling at elevated temperatures of PVDF-PMMA blends

Previous results demonstrate (i) the importance of P_r on piezoelectric coefficients d_{33} and (ii) the occurrence of crystal transformations during the high-voltage AC poling (controlling the final β-/α_p-phase contents and the resulting P_r). The use of PMMA-MAA also induces higher ferroelectric properties and the presence of ionizable moieties is also expected to modify the dielectric behavior of the resulting blend, in particular at elevated temperatures where ionic conduction mechanisms could be activated. In this respect, high-voltage AC poling experiments were carried out at elevated temperatures (75°C) to boost ferroelectric properties via the specific use of PMMA-MAA. (P-E)/(I-E) hysteresis loops at 75 ºC for neat PVDF, PVDF/PMMA and PVDF/PMMA-MAA blends (5 wt-% additives) are displayed in **Figure 7**. Quantitative information (P_r, E_c and ferroelectric quality factors) are given in the Supporting Information section (**Table SI2**).

High-voltage poling at 75 °C significantly enhances the ferroelectric switching behavior of PVDF/PMMA and PVDF/PMMA-MAA blends and very high remanent polarizations close to 6.7 – 7.0 μC/cm² were achieved, respectively (**Table SI2**). PVDF/PMMA and PVDF/PMMA-MAA display similar ferroelectric properties but slightly better performances are obtained with PMMA-MAA. Both materials show square (P-E) loops with nearly-saturated polarization and ferroelectric quality factors close to 1 indicating the absence of dipole relaxation. (I-E) curves also indicate fairly-homogenous dipole switching. The high-quality ferroelectric loops with large P_r and low E_c are quite similar to recent studies on PVDF-TrFE films poled under similar conditions[57]. Interestingly, ab initio studies indicate a maximal spontaneous polarization of about 18.8 μC/cm²

for PVDF β-crystals[61,62]. Considering the maximum amount of β-phase achieved after high-voltage poling (close to 40%), the maximal remanent polarization attainable would be about 7.5 μC/cm² in our materials (which can be enhanced to about 8.5 μC/cm² in the case of full α-to-α_p-to-β crystals conversion with a final β-phase content of 45%). In this context, the high-voltage poling process at elevated temperature clearly enables a nearly-perfect poling of β-crystals in PVDF/PMMA-MAA to reach high P_r values close to the theoretical limit value. Potential piezoelectric coefficients up to 16 pC/N are expected (according to **Figure 5**).

Neat PVDF also shows the same positive trend regarding the impact of the poling temperature on the ferroelectric switching behavior and remanent polarizations up to 3.8 μC/cm² were achieved at 75°C (**Table SI2**). However, (P-E) loops are still far from polarization saturation with a reduced ferroelectric quality factor and (I-E) curves indicate inhomogeneous switching with a very broad distribution of coercive fields. Such effects are in accordance with an enhanced amorphous phase mobility inducing a reduced dipole coupling due to dipole relaxation within the amorphous phase[63,64]. In this respect, the use of PMMA and in particular PMMA-MAA is clearly crucial to enable a nearly-perfect poling of β-crystals at elevated poling temperature with high P_r values and to produce high-quality ferroelectric behaviors.

The origin of such high-quality ferroelectric behaviors obtained at elevated poling temperature still remain complex to identify but PMMA and PMMA-MAA is suspected to activate peculiar ionic conduction mechanisms inside the amorphous phase that enhance/stabilize charge compensation effects and/or modify the effective internal electric field. Such modifications of the ionic conductivity has been already detected in PVDF/PMMA blends with an increase of the electrical conductivity from approx. $0.8 – 200.10^{-15}$ S/cm between 23 °C and 90 °C respectively (compared to $5 – 700.10^{-15}$ S/cm in the case of neat PVDF)[65]. Such conclusions are also in

agreement with the ionic nature of PMMA-MAA that naturally bring new conduction mechanisms, in particular at elevated temperature.

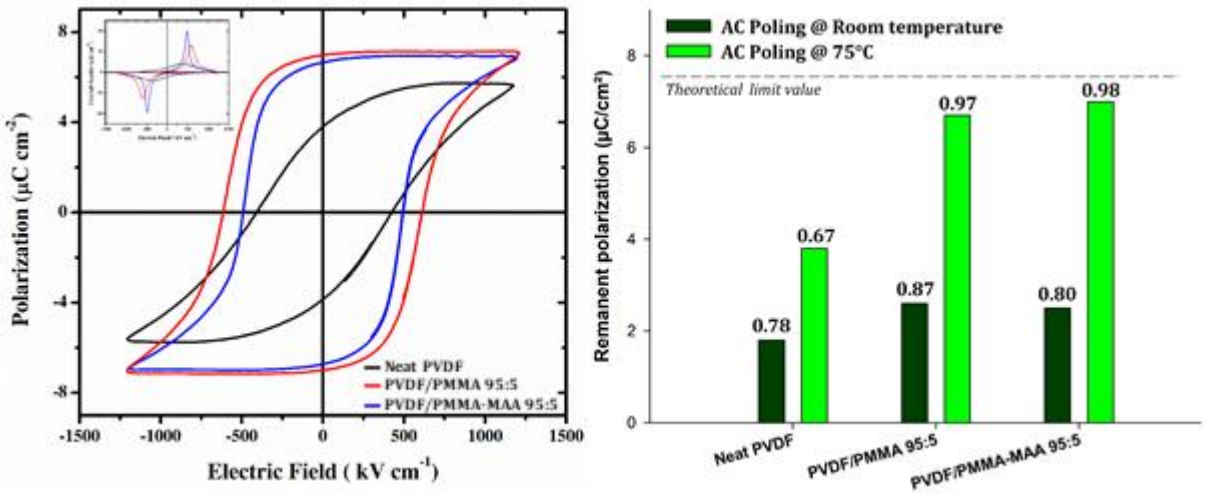

Figure 7. (P-E) loops recorded at 75°C for neat PVDF (black), PVDF/PMMA 95:5 (blue) and PVDF/PMMA-MAA 95:05 (red) blends processed into films by extrusion-calendering (left). Corresponding (I-E) curves in the insert. Subsequent impact of poling temperature on remanent polarization of as-produced films (AC electrical field 1200 kV/cm, film thickness 25-35 μm, ferroelectric quality factor P_r/P_{sat} into brackets) (right).

In conclusion, high-voltage AC poling at elevated temperatures clearly represents an interesting approach to boost ferroelectric and piezoelectric performances of melt-processed PVDF-based blends using functional PMMA-MAA additives in low amounts. The use of PMMA-MAA (an even PMMA) is clearly crucial to enable a nearly-perfect poling of β-crystals at elevated poling temperature and to produce high-quality ferroelectric behaviors with high P_r values up to the theoretical limit value. Several hypotheses need to be tested in a near future, in particular (i) the impact of the high-voltage poling temperature on the α-to-α_p-to-β crystal transformation, (ii) the role of the electrical conductivity on charge compensation/trapping/stabilization (in PVDF/PMMA

blends) and (iii) the role of dipole relaxation within the amorphous phase. The time-temperature stability of ferroelectric/piezoelectric behavior induced by high-voltage poling at elevated temperatures also need further investigations for practical applications.

4. Conclusions

PVDF/PMMA-MAA blends were processed into thin films by an industrially-relevant melt-state extrusion-calendering and several characterizations were conducted to identify the role of PMMA-MAA on β-phase crystallization and subsequent ferro/piezoelectric properties. FDSC experiments highlight a good miscibility between PVDF and PMMA-MAA. The PMMA-MAA copolymer acts as a PVDF β-phase promoter with a slightly better efficiency than PMMA (slight shift of α-to-β crystal transition towards lower cooling rates compared to the corresponding blends with PMMA). A transposition to melt-processed PVDF-based blends by extrusion-calendering is attempted and ATR-FTIR/WAXS analysis attested for an intensive production of the PVDF β-phase in PVDF/PMMA-MAA with a specific incorporation of 5 wt-% PMMA-MAA. In this respect, thin films based on PVDF/PMMA-MAA with high amounts in polar crystals (β-phase fraction up to 80%, β-phase crystallinity up to 35 %) could be produced by an industrially-relevant melt extrusion-calendering process and this blend seems to be a promising ferroelectric/piezoelectric material. However, the amount of PMMA-MAA should be limited to 5 wt-% due demixing phenomena at higher PMMA-MAA loadings. Discrepancies are observed with FDSC analysis that indicate peculiar effects of the extrusion-calendering processing (shearing/pressure-induced demixing) on the β-phase crystallization.

Ferroelectric properties at room temperature were established for PVDF/PMMA-MAA blends processed by extrusion-calendering using (P-E)/(I-E) hysteresis loops. The best performances are observed with the incorporation of 5 wt-% PMMA-MAA with a P_r value up to 4.9 μC/cm² using a

AC electric field of 1500 kV/cm (value close to stretched PVDF). This effect seems to arise from the enhanced β-phase content for this specific formulation. Piezoelectric properties were also improved at an optimal content of 5 wt-% PMMA or PMMA-MAA with a maximal value close to 11 pC/N. A clear linear relationship between P_r and d_{33} has been demonstrated confirming the importance of ferroelectric properties to optimize piezoelectric properties of PVDF/PMMA blends. Despite higher initial β-phase content in PVDF/PMMA-MAA, only modest improvements were noticed for PVDF/PMMA-MAA blends compared to PVDF/PMMA blends.

Finally, a complex crystal transformation occurs during high-voltage poling, in accordance with a α-to-α_p-to-β crystal transformation pathway. A maximal amount of β-phase close to 38 – 39 % is obtained with the specific use of 5 wt-% PMMA or PMMA-MAA. The role of the α_p-phase is indirectly evidenced, in particular for neat PVDF. Finally, high-voltage poling at elevated temperatures (up to 75°C) could significantly improve ferroelectric performances and qualities of the PVDF/PMMA-MAA blend (P_r values up to 7.0 μC/cm²). PVDF/PMMA blend also shows interesting (but lower) ferroelectric properties that demonstrates the crucial role of PMMA-MAA combined to high-voltage poling at elevated temperatures. This copolymer clearly enable a nearly-perfect poling of β-crystals at elevated poling temperature to produce high-quality ferroelectric behaviors with high P_r values up to the theoretical limit value (and with theoretical piezoelectric coefficients d_{33} up to 16 pC/N). Underlying phenomena still request in-depth investigations in a near future on various scientific/technological aspects (impact of the shearing on the α-to-β crystal crystallization, precise α-to-α_p-to-β crystal transformation pathway, role of the electrical conductivity and dipole relaxation within the amorphous phase on charge trapping/stabilization, time-temperature stability of ferroelectric/piezoelectric performances). However, this study clearly demonstrates that PVDF blends with miscible functional PMMA copolymers such as PMMA-

MAA consequently represent an interesting approach to develop cost-effective electroactive polymer materials for advanced ferro/piezoelectric devices using industrially-relevant processes.

Supporting Information.

Figure SI1: Crystallization temperatures for α- & β-crystals detected by FDSC as a function of the cooling rate for neat PVDF, PVDF/PMMA with 5 wt-% PMMA, PVDF/PMMA with 10 wt-% PMMA, PVDF/PMMA-MAA blends with 5 wt-% PMMA-MAA and PVDF/PMMA-MAA blends with 10 wt-% PMMA-MAA. **Figure SI2** : Full ATR-FTIR spectra of PVDF/PMMA and PVDF/PMMA-MAA blends processed into films by extrusion-calendering. **Figure SI3** : Optical inspections of PVDF/PMMA and PVDF/PMMA-MAA blends processed into films by extrusion-calendering and corresponding 2D-SAXS spectra. **Figure SI4.** (I-E) hysteresis loops under increasing AC electric fields for PVDF/PMMA and PVDF/PMMA-MAA blends processed into films by extrusion-calendering. **Table SI1.** Time stability of the piezoelectric coefficient d_{33} for PVDF/PMMA and PVDF/PMMA-MAA blends processed into films by extrusion-calendering. **Table SI2.** Remanent polarization and coercive electric field as a function of the high-voltage poling temperature for PVDF-based blends with PMMA and PMMA-MAA processed into films by extrusion-calendering calendering.

The following files are available free of charge. File type PDF.

Corresponding Author.

*Dr. Cedric Samuel (cedric.samuel@imt-lille-douai.fr)

Author Contributions

The manuscript was written through contributions of all authors. All authors have given approval to the final version of the manuscript. All authors contributed equally.

Funding Sources

European Commission (FEDER, INTERREG V FWVL program, BIOHARV project, GoToS3 portofolio), Hauts-de-France Region (France), Wallonia Region/Service Public de Wallonie (Belgium), West Vlaanderen Region (Belgium), Agentschap Innoveren Ondernemen (Belgium), Belgian Federal Government Office of Science Policy/Belgian Federal Science Policy Office (SSTC – PAI 6/27, Belgium), International Campus on Safety and Intermodality in Transportation (CISIT, France), Ministerio de Economía y Competitividad (MINECO, projects MAT2017-88788-R and MAT2016-76851-R, Spain).

Acknowledgments

Authors gratefully acknowledge the Wallonia Region/Service Public de Wallonie (Belgium), West Vlaanderen Region (Belgium), Agentschap Innoveren Ondernemen (Belgium) and European Commission (FEDER) for the financial support in the framework of the INTERREG V FWVL program (BIOHARV project, GoToS3 portofolio). Authors particularly thank Samuel Devisme from Arkema (France) for supplying raw materials. UMons (LPCM) gratefully acknowledges the Belgian Federal Government Office of Science Policy/Belgian Federal Science Policy Office (SSTC – PAI 6/27, Belgium) for general support and is much indebted to both the Wallonia Region/Service Public de Wallonie (Belgium) and the European Commission (FEDER) for financial support in the frame of phasing-out Hainaut. IMT Lille Douai and Université de Lille acknowledge both the International Campus on Safety and Intermodality in Transportation (CISIT, France), the Hauts-de-France Region (France) and the European Commission (FEDER) for their contributions to funding extrusion equipments, SAXS-WAXS laboratory equipments and calorimetric characterization tools. Authors also thanks the Spanish Ministerio de Economía y

Competitividad (MINECO) for financial supports of MAT2017-88788-R and MAT2016-76851-R projects.

References

(1) Ameduri, B. From Vinylidene Fluoride (VDF) to the Applications of VDF-Containing Polymers and Copolymers: Recent Developments and Future Trends. *Chem. Rev.* **2009**, *109* (12), 6632–6686. https://doi.org/10.1021/cr800187m.

(2) Martins, P.; Lopes, A. C.; Lanceros-Mendez, S. Electroactive Phases of Poly(Vinylidene Fluoride): Determination, Processing and Applications. *Prog. Polym. Sci.* **2014**, *39* (4), 683–706. https://doi.org/10.1016/j.progpolymsci.2013.07.006.

(3) Murayama, N.; Nakamura, K.; Obara, H.; Segawa, M. The Strong Piezoelectricity in Polyvinylidene Fluroide (PVDF). *Ultrasonics* **1976**, *14* (1), 15–24. https://doi.org/10.1016/0041-624x(76)90067-6.

(4) Kepler, R. G.; Anderson, R. A. Ferroelectricity in Polyvinylidene Fluoride. *J. Appl. Phys.* **1978**, *49* (3), 1232–1235. https://doi.org/10.1063/1.325011.

(5) Stadlober, B.; Zirkl, M.; Irimia-Vladu, M. Route towards Sustainable Smart Sensors: Ferroelectric Polyvinylidene Fluoride-Based Materials and Their Integration in Flexible Electronics. *Chem. Soc. Rev.* **2019**, *48* (6), 1787–1825. https://doi.org/10.1039/c8cs00928g.

(6) Vatansever, D.; Hadimani, R. L.; Shah, T.; Siores, E. An Investigation of Energy Harvesting from Renewable Sources with PVDF and PZT. *Smart Mater. Struct.* **2011**, *20* (5), 55019. https://doi.org/10.1088/0964-1726/20/5/055019.

(7) Shepelin, N. A.; Glushenkov, A. M.; Lussini, V. C.; Fox, P. J.; Dicinoski, G. W.; Shapter,

J. G.; Ellis, A. V. New Developments in Composites, Copolymer Technologies and Processing Techniques for Flexible Fluoropolymer Piezoelectric Generators for Efficient Energy Harvesting. *Energy Environ. Sci.* **2019**, *12* (4), 1143–1176. https://doi.org/10.1039/c8ee03006e.

(8) Zhu, L. Exploring Strategies for High Dielectric Constant and Low Loss Polymer Dielectrics. *J. Phys. Chem. Lett.* **2014**, *5* (21), 3677–3687. https://doi.org/10.1021/jz501831q.

(9) Zhu, L.; Wang, Q. Novel Ferroelectric Polymers for High Energy Density and Low Loss Dielectrics. *Macromolecules* **2012**, *45* (7), 2937–2954. https://doi.org/10.1021/ma2024057.

(10) Jones, R. E.; Maniar, P. D.; Moazzami, R.; Zurcher, P.; Witowski, J. Z.; Lii, Y. T.; Chu, P.; Gillespie, S. J. Ferroelectric Non-Volatile Memories for Low-Voltage, Low-Power Applications. *Thin Solid Films* **1995**, *270* (1–2), 584–588. https://doi.org/10.1016/0040-6090(95)06754-X.

(11) Das, S.; Appenzeller, J. FETRAM. An Organic Ferroelectric Material Based Novel Random Access Memory Cell. *Nano Lett.* **2011**, *11* (9), 4003–4007. https://doi.org/10.1021/nl2023993.

(12) Kang, S. J.; Park, Y. J.; Bae, I.; Kim, K. J.; Kim, H. C.; Bauer, S.; Thomas, E. L.; Park, C. Printable Ferroelectric PVDF/PMMA Blend Films with Ultralow Roughness for Low Voltage Non-Volatile Polymer Memory. *Adv. Funct. Mater.* **2009**, *19* (17), 2812–2818. https://doi.org/10.1002/adfm.200900589.

(13) Jeon, J. H.; Kang, S. P.; Lee, S.; Oh, I. K. Novel Biomimetic Actuator Based on SPEEK

and PVDF. *Sensors Actuators, B Chem.* **2009**, *143* (1), 357–364. https://doi.org/10.1016/j.snb.2009.09.020.

(14) Mohammadi, B.; Yousefi, A. A.; Bellah, S. M. Effect of Tensile Strain Rate and Elongation on Crystalline Structure and Piezoelectric Properties of PVDF Thin Films. *Polym. Test.* **2007**, *26* (1), 42–50. https://doi.org/10.1016/j.polymertesting.2006.08.003.

(15) Hahn, B. R.; Wendorff, J. H. Piezo- and Pyroelectricity in Polymer Blends of Poly(Vinylidene Fluoride)/Poly(Methyl Methacrylate). *Polymer* **1985**, *26* (11), 1611–1618. https://doi.org/10.1016/0032-3861(85)90272-1.

(16) Bharti, V.; Kaura, T.; Nath, R. Ferroelectric Hysteresis in Simultaneously Stretched and Corona-Poled PVDF Films. *IEEE Trans. Dielectr. Electr. Insul.* **1997**, *4* (6), 738–741. https://doi.org/10.1109/94.654689.

(17) Gomes, J.; Nunes, J. S.; Sencadas, V.; Lanceros-Mendez, S. Influence of the β-Phase Content and Degree of Crystallinity on the Piezo- and Ferroelectric Properties of Poly(Vinylidene Fluoride). *Smart Mater. Struct.* **2010**, *19* (6), 065010. https://doi.org/10.1088/0964-1726/19/6/065010.

(18) Das-Gupta, D. K.; Doughty, K. Corona Charging and the Piezoelectric Effect in Polyvinylidene Fluoride. *J. Appl. Phys.* **1978**, *49* (8), 4601–4603. https://doi.org/10.1063/1.325441.

(19) Hahn, B.; Wendorff, J.; Yoon, D. Y. Dielectric Relaxation of the Crystal-Amorphous Interphase in Poly(Vinylidene Fluoride) and Its Blends with Poly(Methyl Methacrylate). *Macromolecules* **1985**, *18* (4), 718–721. https://doi.org/10.1021/ma00146a024.

(20) Hahn, B. R.; Herrmann-Schönherr, O.; Wendorff, J. H. Evidence for a Crystal-Amorphous Interphase in PVDF and PVDF/PMMA Blends. *Polymer* **1987**, *28* (2), 201–208. https://doi.org/10.1016/0032-3861(87)90404-6.

(21) Martins, P.; Nunes, J. S.; Hungerford, G.; Miranda, D.; Ferreira, A.; Sencadas, V.; Lanceros-Méndez, S. Local Variation of the Dielectric Properties of Poly(Vinylidene Fluoride) during the α- to β-Phase Transformation. *Phys. Lett. Sect. A Gen. At. Solid State Phys.* **2009**, *373* (2), 177–180. https://doi.org/10.1016/j.physleta.2008.11.026.

(22) Lund, A.; Gustafsson, C.; Bertilsson, H.; Rychwalski, R. W. Enhancement of β Phase Crystals Formation with the Use of Nanofillers in PVDF Films and Fibres. *Compos. Sci. Technol.* **2011**, *71* (2), 222–229. https://doi.org/10.1016/j.compscitech.2010.11.014.

(23) Mishra, S.; Kumaran, K. T.; Sivakumaran, R.; Pandian, S. P.; Kundu, S. Synthesis of PVDF/CNT and Their Functionalized Composites for Studying Their Electrical Properties to Analyze Their Applicability in Actuation & Sensing. *Colloids Surfaces A Physicochem. Eng. Asp.* **2016**, *509*, 684–696. https://doi.org/10.1016/j.colsurfa.2016.09.007.

(24) Ke, K.; Pötschke, P.; Jehnichen, D.; Fischer, D.; Voit, B. Achieving β-Phase Poly(Vinylidene Fluoride) from Melt Cooling: Effect of Surface Functionalized Carbon Nanotubes. *Polymer* **2014**, *55* (2), 611–619. https://doi.org/10.1016/j.polymer.2013.12.014.

(25) Sencadas, V.; Lanceros-Méndez, S.; Mano, J. F. Characterization of Poled and Non-Poled β-PVDF Films Using Thermal Analysis Techniques. *Thermochim. Acta* **2004**, *424* (1–2), 201–207. https://doi.org/10.1016/j.tca.2004.06.006.

(26) Léonard, C.; Halary, J. L.; Monnerie, L. Hydrogen Bonding in PMMA-Fluorinated Polymer

Blends: FTi.r. Investigations Using Ester Model Molecules. *Polymer* **1985**, *26* (10), 1507–1513. https://doi.org/10.1016/0032-3861(85)90084-9.

(27) Li, M.; Stingelin, N.; Michels, J. J.; Spijkman, M. J.; Asadi, K.; Feldman, K.; Blom, P. W. M.; De Leeuw, D. M. Ferroelectric Phase Diagram of PVDF:PMMA. *Macromolecules* **2012**, *45* (18), 7477–7485. https://doi.org/10.1021/ma301460h.

(28) Sasaki, H.; Kanti Bala, P.; Yoshida, H.; Ito, E. Miscibility of PVDF/PMMA Blends Examined by Crystallization Dynamics. *Polymer* **1995**, *36* (25), 4805–4810. https://doi.org/10.1016/0032-3861(95)99296-7.

(29) Okabe, Y.; Murakami, H.; Osaka, N.; Saito, H.; Inoue, T. Morphology Development and Exclusion of Noncrystalline Polymer during Crystallization in PVDF/PMMA Blends. *Polymer* **2010**, *51* (6), 1494–1500. https://doi.org/10.1016/j.polymer.2010.01.055.

(30) Linares, A.; Acosta, J. L. Tensile and Dynamic Mechanical Behaviour of Polymer Blends Based on PVDF. *Eur. Polym. J.* **1997**, *33* (4), 467–473. https://doi.org/10.1016/S0014-3057(96)00182-6.

(31) Domenici, C.; De Rossi, D.; Nannini, A.; Verni, R. Piezoelectric Properties and Dielectric Losses in PVDF-PMMA Blends. *Ferroelectrics* **1984**, *60* (1), 61–70. https://doi.org/10.1080/00150198408017510.

(32) Léonard, C.; Halary, J. L.; Monnerie, L. Crystallization of Poly(Vinylidene Fluoride)-Poly(Methyl Methacrylate) Blends: Analysis of the Molecular Parameters Controlling the Nature of the Poly(Vinylidene Fluoride) Crystalline Phase. *Macromolecules* **1988**, *21* (10), 2988–2994. https://doi.org/10.1021/ma00188a016.

(33) De Neef, A.; Samuel, C.; Stoclet, G.; Rguiti, M.; Courtois, C.; Dubois, P.; Soulestin, J.; Raquez, J. M. Processing of PVDF-Based Electroactive/Ferroelectric Films: Importance of PMMA and Cooling Rate from the Melt State on the Crystallization of PVDF Beta-Crystals. *Soft Matter* **2018**, *14* (22), 4591–4602. https://doi.org/10.1039/c8sm00268a.

(34) Wang, Y. D.; Cakmak, M. Hierarchical Structure Gradients Developed in Injection- molded PVDF and PVDF–PMMA Blends. I. Optical and Thermal Analysis. *J. Appl. Polym. Sci.* **1998**, *68* (6), 909–926. https://doi.org/10.1002/(sici)1097-4628(19980509)68:6<909::aid-app5>3.3.co;2-d.

(35) Zhao, X.; Chen, S.; Zhang, J.; Zhang, W.; Wang, X. Crystallization of PVDF in the PVDF/PMMA Blends Precipitated from Their Non-Solvents: Special Orientation Behavior, Morphology, and Thermal Properties. *J. Cryst. Growth* **2011**, *328* (1), 74–80. https://doi.org/10.1016/j.jcrysgro.2011.06.036.

(36) Gradys, A.; Sajkiewicz, P.; Adamovsky, S.; Minakov, A.; Schick, C. Crystallization of Poly(Vinylidene Fluoride) during Ultra-Fast Cooling. *Thermochim. Acta* **2007**, *461* (1–2), 153–157. https://doi.org/10.1016/j.tca.2007.05.023.

(37) Mackey, M.; Schuele, D. E.; Zhu, L.; Flandin, L.; Wolak, M. A.; Shirk, J. S.; Hiltner, A.; Baer, E. Reduction of Dielectric Hysteresis in Multilayered Films via Nanoconfinement. *Macromolecules* **2012**, *45* (4), 1954–1962. https://doi.org/10.1021/ma202267r.

(38) Yang, X.; Kong, X.; Tan, S.; Li, G.; Ling, W.; Zhou, E. Spatially-Confined Crystallization of Poly(Vinylidene Fluoride). *Polym. Int.* **2000**, *49* (11), 1525–1528. https://doi.org/10.1002/1097-0126(200011)49:11<1525::AID-PI563>3.0.CO;2-I.

(39) Oikonomou, E. K.; Tencé-Girault, S.; Gérard, P.; Norvez, S. Swelling of Semi-Crystalline PVDF by a PMMA-Based Nanostructured Diblock Copolymer: Morphology and Mechanical Properties. *Polymer* **2015**, *76*, 89–97. https://doi.org/10.1016/j.polymer.2015.08.055.

(40) Wang, P.; Xu, P.; Zhou, Y.; Yang, Y.; Ding, Y. Effect of MWCNTs and P[MMA-IL] on the Crystallization and Dielectric Behavior of PVDF Composites. *Eur. Polym. J.* **2018**, *99* (April 2017), 58–64. https://doi.org/10.1016/j.eurpolymj.2017.12.003.

(41) Xiao, Q.; Wang, X.; Li, W.; Li, Z.; Zhang, T.; Zhang, H. Macroporous Polymer Electrolytes Based on PVDF/PEO-b-PMMA Block Copolymer Blends for Rechargeable Lithium Ion Battery. *J. Memb. Sci.* **2009**, *334* (1–2), 117–122. https://doi.org/10.1016/j.memsci.2009.02.018.

(42) Li, H.; Lin, C. E.; Shi, J. L.; Ma, X. T.; Zhu, B. K.; Zhu, L. P. Preparation and Characterization of Safety PVDF/P(MMA-Co-PEGMA) Active Separators by Studying the Liquid Electrolyte Distribution in This Kind of Membrane. *Electrochim. Acta* **2014**, *115*, 317–325. https://doi.org/10.1016/j.electacta.2013.10.183.

(43) Tu, K.; Shen, P.; Li, J.; Fan, B.; Yang, C.; Du, R. Preparation of Enduringly Antifouling PVDF Membrane with Compatible Zwitterionic Copolymer via Thermally Induced Phase Separation. *J. Appl. Polym. Sci.* **2015**, *132* (7), 1–6. https://doi.org/10.1002/app.41362.

(44) Wang, L.; Chen, S. Crystallization Behaviors of Poly(Vinylidene Fluoride) and Poly(Methyl Methacrylate)-Block-Poly(2-Vinyl Pyridine) Block Copolymer Blends. *J. Therm. Anal. Calorim.* **2016**, *125* (1), 215–230. https://doi.org/10.1007/s10973-016-5364-3.

(45) Gong, H.; Miao, B.; Zhang, X.; Lu, J.; Zhang, Z. High-Field Antiferroelectric-like Behavior in Uniaxially Stretched Poly(Vinylidene Fluoride-Trifluoroethylene-Chlorotrifluoroethylene)-Grafted-Poly(Methyl Methacrylate) Films with High Energy Density. *RSC Adv.* **2016**, *6* (2), 1589–1599. https://doi.org/10.1039/c5ra22617a.

(46) Li, J.; Gong, H.; Yang, Q.; Xie, Y.; Yang, L.; Zhang, Z. Linear-like Dielectric Behavior and Low Energy Loss Achieved in Poly(Ethyl Methacrylate) Modified Poly(Vinylidene-Co-Trifluoroethylene). *Appl. Phys. Lett.* **2014**, *104* (26), 263901. https://doi.org/10.1063/1.4886391.

(47) Guan, F.; Wang, J.; Yang, L.; Tseng, J. K.; Han, K.; Wang, Q.; Zhu, L. Confinement-Induced High-Field Antiferroelectric-like Behavior in a Poly(Vinylidene Fluoride-Co-Trifluoroethylene-Co-Chlorotrifluoroethylene)-Graft-Polystyrene Graft Copolymer. *Macromolecules* **2011**, *44* (7), 2190–2199. https://doi.org/10.1021/ma102910v.

(48) Gregorio, R.; Cestari, M. Effect of Crystallization Temperature on the Crystalline Phase Content and Morphology of Poly(Vinylidene Fluoride). *J. Polym. Sci. Part B Polym. Phys.* **1994**, *32* (5), 859–870. https://doi.org/10.1002/polb.1994.090320509.

(49) Amorín, H.; Jiménez, R.; Deluca, M.; Ricote, J.; Hungría, T.; Castro, A.; Algueró, M. Nanostructuring Effects in Piezoelectric BiScO3 -PbTiO 3 Ceramics . *J. Am. Ceram. Soc.* **2014**, *97* (9), 2802–2809. https://doi.org/10.1111/jace.13000.

(50) Amorín, H.; Jiménez, R.; Ricote, J.; Hungría, T.; Castro, A.; Algueró, M. Apparent Vanishing of Ferroelectricity in Nanostructured $BiScO_3$-$PbTiO_3$. *J. Phys. D. Appl. Phys.* **2010**, *43* (28), 285401–285406. https://doi.org/10.1088/0022-3727/43/28/285401.

(51) Qiu, X.; Holländer, L.; Wirges, W.; Gerhard, R.; Cury Basso, H. Direct Hysteresis Measurements on Ferroelectret Films by Means of a Modified Sawyer-Tower Circuit. *J. Appl. Phys.* **2013**, *113* (22), 224106. https://doi.org/10.1063/1.4809556.

(52) Landis, F. A.; March, S. R.; Deivasagayam, D.; Mathers, R. T. Crystallization of Poly(Vinylidene Fluoride) in Blends with Poly(Methyl Methacrylate-Co-Methacrylic Acid) Copolymers. *Macromol. Chem. Phys.* **2014**, *215* (2), 153–162. https://doi.org/10.1002/macp.201300535.

(53) Salimi, A.; Yousefi, A. A. FTIR Studies of β-Phase Crystal Formation in Stretched PVDF Films. *Polym. Test.* **2003**, *22* (6), 699–704. https://doi.org/10.1016/S0142-9418(03)00003-5.

(54) Ramadan, K. S.; Sameoto, D.; Evoy, S. A Review of Piezoelectric Polymers as Functional Materials for Electromechanical Transducers. *Smart Mater. Struct.* **2014**, *23* (3), 033001. https://doi.org/10.1088/0964-1726/23/3/033001.

(55) Kanik, M.; Aktas, O.; Sen, H. S.; Durgun, E.; Bayindir, M.; Science, M. Spontaneous High Piezoelectricity in Poly (Vinylidene Fluoride) Nanoribbons. *ACS Nano* **2014**, *8* (9), 9311–9323. https://doi.org/10.1021/nn503269b.

(56) Furukawa, T.; Lovinger, A. J.; Broadhurst, M. G.; Davis, G. T. Dielectric Hysteresis and Nonlinearity in a 52/48 Mol % Copolymer of Vinylidene Fluoride and Trifluoroethylene. *Macromolecules* **1983**, *16* (12), 1885–1890. https://doi.org/10.1021/ma00246a015.

(57) Liu, Y.; Aziguli, H.; Zhang, B.; Xu, W.; Lu, W.; Bernholc, J.; Wang, Q. Ferroelectric Polymers Exhibiting Behaviour Reminiscent of a Morphotropic Phase Boundary. *Nature*

2018, *562* (7725), 96–100. https://doi.org/10.1038/s41586-018-0550-z.

(58) Davies, G. R.; Singh, H. Evidence for a New Crystal Phase in Conventionally Poled Samples of Poly(Vinylidene Fluoride) in Crystal Form II. *Polymer* **1979**, *20* (6), 772–774. https://doi.org/10.1016/0032-3861(79)90253-2.

(59) Davis, G. T.; McKinney, J. E.; Broadhurst, M. G.; Roth, S. C. Electric-Field-Induced Phase Changes in Poly(Vinylidene Fluoride). *J. Appl. Phys.* **1978**, *49* (10), 4998–5002. https://doi.org/10.1063/1.324446.

(60) Bormashenko, Y.; Pogreb, R.; Stanevsky, O.; Bormashenko, E. Vibrational Spectrum of PVDF and Its Interpretation. *Polym. Test.* **2004**, *23* (7), 791–796. https://doi.org/10.1016/j.polymertesting.2004.04.001.

(61) Nakhmanson, S. M.; Nardelli, M. B.; Bernholc, J. Ab Initio Studies of Polarization and Piezoelectricity in Vinylidene Fluoride and BN-Based Polymers. *Phys. Rev. Lett.* **2004**, *92* (11). https://doi.org/10.1103/PhysRevLett.92.115504.

(62) Nakhmanson, S. M.; Nardelli, M. B.; Bernholc, J. Collective Polarization Effects in β-Polyvinylidene Fluoride and Its Copolymers with Tri- and Tetrafluoroethylene. *Phys. Rev. B - Condens. Matter Mater. Phys.* **2005**, *72* (11), 115210. https://doi.org/10.1103/PhysRevB.72.115210.

(63) Teyssedre, G.; Grimau, M.; Bernes, A.; Martinez, J. J.; Lacabanne, C. α-Relaxation/Retardation Mode in Semicrystalline Polymers with Flexible Chains. *Polymer* **1994**, *35* (20), 4397–4403. https://doi.org/10.1016/0032-3861(94)90098-1.

(64) Teyssedre, G.; Bernes, A.; Lacabanne, C. Influence of the Crystalline Phase on the

Molecular Mobility of PVDF. *J. Polym. Sci. Part B Polym. Phys.* **1993**, *31* (13), 2027–2034. https://doi.org/10.1002/polb.1993.090311316.

(65) Becker, A.; Stein, M.; Jungnickel, B. J. Dependence on Supermolecular Structure and on Charge Injection Conditions of Ferroelectric Switching of Pvdf and Its Blends with PMMA. *Ferroelectrics* **1995**, *171* (1), 111–123. https://doi.org/10.1080/00150199508018426.